Low Cost ATP System Design for Free Space Optics based Drone Assisted Wireless Networks

Xiang Sun*, Tianrun Zhang*, Sihua Shao[†], Bryan Tice*, Paul Tice*, and Sudharman Jayaweera*
*Department of Electrical and Computer Engineering, University of New Mexico, Albuquerque, NM 87131, USA.

†Department of Electrical Engineering, New Mexico Tech, Socorro, NM 87801, USA.

Abstract-In a drone assisted wireless network, a drone is deployed over a place of interest (PoI) to relay traffic between the users at the PoI and a nearby wireless access point (WAP). To alleviate the bottleneck in the fronthaul link between the drone and the WAP, free space optics (FSO) is applied as the fronthaul communications solution. However, due to the mobility of the drone, a low cost and lightweight Acquisition, Tracking, and Pointing (ATP) system is required to ensure the low pointing loss for the FSO based fronthaul link. Although many highaccurate ATP systems have been designed for the FSO system to achieve, for example, ground-to-satellite communications, these ATP systems have high weight and cost, and so may not be suitable to be applied in the drone assisted wireless network, which may not require such high pointing accuracy. In this paper, we design and implement a novel low cost and lightweight gimbalbased ATP system to mitigate the pointing loss for the FSO based fronthaul link in a drone assisted wireless network. We experimentally evaluate the performance of the ATP system and observe that the designed ATP system can have a low pointing loss of the FSO based fronthaul system, especially when the drone is at a low speed with a proper beam divergence angle.

Index Terms-Free space optics, ATP, drone.

I. INTRODUCTION

Vast wireless access points (WAPs) deployment provides almost seamless wireless connections and Internet services to users. However, current wireless networks are vulnerable to natural disasters and burst traffic d emands [1], [2]. For example, a football stadium (when a football game is happening) may become a hotspot area, where many users may generate massive traffic to stress nearby WAPs that may not be able to provide sufficient c apacity [3]. A lso, when a natural disaster strikes an area where all the networks and power infrastructures could be severely damaged, the victims in the disaster struck area cannot communicate with the first responders to conduct effective rescues [4]–[6].

To improve resilience of wireless networks in handling the burst traffic demands and emergency communications, drone assisted wireless networks have been proposed, where a drone is equipped with a small cell base station or a portable WAP to quickly and flexibly be deployed over any places of interest (PoI), such as sporadic hotspots and disaster struck areas [7], [8]. As shown in Fig. 1, the drone is a flying n ode to relay traffic between the users and a WAP. A drone can be deployed

This work was supported by the National Science Foundation under Award CNS-2148178.

close to the users to provide high-speed wireless links. Yet, due to the long distance and high traffic load, the fronthaul link between the drone and the WAP may become the bottleneck to significantly reduce the network throughput. To alleviate the bottleneck, free space optics (FSO) is applied as the fronthaul solution [9]–[11], where an optical beam is transmitted from an FSO transmitter at the WAP to an FSO receiver at the drone carrying data streams. Compared to RF communications, FSO has the following advantages. 1) FSO has a higher link capacity over a longer distance. For instance, an FSO link can offer a Gbps-Tbps data rate at the distance of several kilometers [12]-[15]. 2) FSO is conducted over unlicensed spectrum [16], thus having no spectrum licensing cost. 3) The spectrum used by FSO does not overlap with that used by RF, thus avoiding the interference from RF communications. 4) FSO is secure as any interception/eavesdropping on an FSO link can be easily identified owing to the fact that FSO applies directional beams with narrow beam divergence [17], [18].



Fig. 1: The FSO based drone assisted wireless network.

One of the major challenges in applying FSO as the fronthaul link in drone assisted wireless networks is high mobility and limited payload/power capacity of the drones. Specifically, FSO is a type of point-to-point communications, and so any misalignment between an FSO transmitter and an FSO receiver may significantly reduce the FSO link capacity. Due to the high mobility of a drone, it is critical to design an Acquisition, Tracking, and Pointing (ATP) system to mitigate the misalignment between the FSO transmitter at the WAP and the FSO receiver at the drone¹. On the other hand, since the drones have very limited payload and power capacity, the ATP system should not increase too much weight or

¹Note that it is necessary to implement two FSO based fronthaul links between the drone and the WAP to achieve full-duplex communications, and so both the drone and WAP should have the same equipment, i,e, an FSO transmitter, an FSO receiver, and the corresponding ATP system. However, to better understand the designed system, we only describe the system for downlink communications from the WAP to the drone.

power at the drone side. Although many high-accurate ATP systems have been designed for the FSO system to achieve, for example, the ground-to-satellite and satellite-to-satellite communications, these ATP systems have high weight and cost, thus not suitable to be applied in drone assisted wireless networks. Moreover, the FSO based fronthaul link does not require such high-accurate ATP due to, for example, the relatively short distance between a WAP and a drone. Motivated by this, we design and experimentally test the performance of a cost effective and lightweight ATP system for FSO based fronthaul communications in drone assisted wireless networks. The major contributions of the paper are listed as follows.

- We design a cost effective and lightweight ATP system, which comprises a beacon at the drone, a camera mounted on a gimbal at the WAP, and a controller at the WAP. We develop a fast but accurate image processing algorithm to derive the relative position of the drone based on the captured image, and employ the proportional integral derivative (PID) algorithm to control the gimbal.
- We experimentally evaluate the performance of the designed ATP system in terms of the beam displacement and pointing loss of the FSO link.
- We observe that the designed ATP system can achieve low pointing loss for the FSO based fronthaul system, especially when the drone is in a low speed with proper beam divergence angle.

The rest of the paper is structured as follows. The related work is summarized in Section II. We explain our designed ATP system in Section III. In Section IV, we describe our experimental setups and analyze the experiment results. Section V provides a summary of the paper.

II. RELATED WORK

ATP is essential in an FSO system if the narrow beams are used to carry data streams. In general, ATP can be classified into gimbal-based, mirror-based, and hybrid. In the gimbal-based ATP system, after deriving the drone's position based on the received beacon signal from the drone, a mechanical rotary gimbal, which carries an FSO transmitter, will adjust its movement in the Pan and Tilt directions to ensure the optical beam from the FSO transmitter can be received by the target. The gimbal-based ATP system can adjust its FSO transmitter over a wide angular range of motion, which is necessary for drone assisted wireless networks since drones may move in a wide space [19], [20]. However, the drawback of the gimbal-based ATP system is low pointing resolution (in the range of μ rad), thus unable to provide accurate movement control [21].

The mirror-based ATP system uses fast steering mirrors (FSMs) to adjust the direction of an optical beam. That is, based on the received beacon from the drone, an FSM would adjust its angle to enable the optical beam to be reflected to the right direction towards the FSO receiver at the drone. As compared to the gimbal-based ATP system, the mirror-based ATP system has limited angular range of motion, which may not be suitable for acquisition and tracking the beacon from the drone [22]. However, due to the high pointing resolution

of an FSM (in the range of sub- μ rad), the mirror-based ATP system has fine-grained and high-speed control [23].

The hybrid ATP system combines the gimbal-based and mirror-based solutions. That is, the mirror-based ATP system is mounted on a rotary gimbal, and so after receiving the beacon signal, the controller would adjust the gimbal's movement to achieve a coarse-grained pointing, and tune the FSM to achieve a fine-grained pointing [24]. As compared to the previous two methods, the hybrid ATP system can provide both wide angular range of motion and high pointing resolution, but it has a higher weight, cost, and power consumption as well as complicated control of coordinating the movement of the gimbal and FSM. Normally, the hybrid ATP has been widely used in the FSO system for long distance communications (e.g., ground-to-satellite and satellite-to-satellite communications) or high-speed train communications [25]. However, the necessity of applying the hybrid ATP to the FSO based fronthaul system in a drone assisted network is still unclear.

In this paper, we implement a new gimbal-based ATP system, where a camera is used to capture the image containing the beacon signal, a fast but accurate image processing algorithm is designed to extract the relative position of the drone, and the PID algorithm is used to control the gimbal based on the derived information. We experimentally evaluate the performance of the ATP system and expect that the designed ATP system can achieve low pointing loss for the FSO based fronthaul system in a drone assisted network, especially when the drone is in a low speed with proper beam divergence angle.

III. SYSTEM MODELS

To achieve high link capacity, the FSO based fronthaul link applies a narrow beam to carry data streams from a WAP to a drone. Hence, any misalignment from an FSO transmitter at the WAP and an FSO receiver at the drone may lead to high pointing loss [26], which can be described as the displacement between the center of the optical beam at the FSO receiver and the center of the FSO receiver's aperture as shown in Fig. 1, thus significantly reducing the link capacity. Denote $d = (d_x, d_y)$ as the corresponding displacement, where d_x and d_y are the displacements in Pan and Tilt, respectively.

To alleviate the pointing loss, ATP is necessary to be used in the FSO based fronthaul system. As shown in Fig. 2, the ATP system comprises a beacon signal (e.g., an infrared light) at the drone, a camera/CMOS sensor mounted on a gimbal at the WAP, and a controller, where the beacon signal is used to indicate the location of the drone, the camera is to capture the image containing the beacon signal from the drone and forward the image to the controller, and the controller is to derive the displacement between the center of the beacon beam and the center of the camera's Field-of-View (FoV), denoted as δ , calculate the corresponding angular velocity of the gimbal based on the PID algorithm, and send the angular velocity to the gimbal, which adjusts its axes accordingly to minimize δ . Specifically, there are four major functions in the controller.

1) **Down sampling**: Once the controller receives an FoV image from the camera with $N \times M$ resolution, it

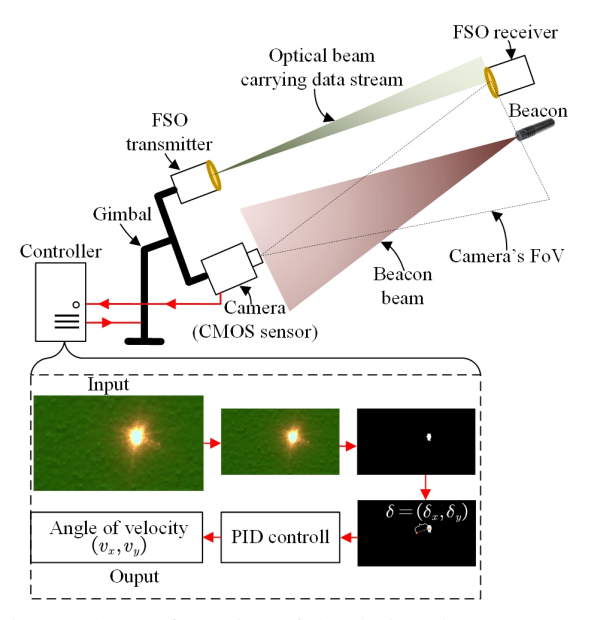


Fig. 2: The configuration of the designed ATP system.

decreases the sample rate of the image by a factor of κ to generate a new FoV image with $N' \times M'$ resolution. The reason of conducting down sampling is to reduce the latency of the image processing in next two steps.

- 2) **Image filtering**: The RGB image is the converted into a binary image, whose pixels have only 0 or 1 intensity values, i.e., $x_{nm} \in \{0,1\}$, where x_{nm} is the intensity value for the pixel in row n $(1 \le n \le N')$ and column m $(1 \le m \le M')$ of the binary image.
- 3) **Identifying the displacement** δ : The beam spot of the beacon in the binary image could be a circle, ellipse, or any irregular shape. Denote (n^*, m^*) as the center of the beam spot for the beacon, which is estimated based on

$$\begin{cases}
n^* = arg \max_{n} \left\{ \sum_{m=1}^{M'} x_{nm} \mid 1 \leqslant n \leqslant N' \right\}, \\
m^* = arg \max_{m} \left\{ \sum_{n=1}^{N'} x_{nm} \mid 1 \leqslant m \leqslant M' \right\}.
\end{cases} (1)$$

Therefore, $\delta=(\delta_x,\delta_y)$, i.e., the displacement (in pixels) between the center of the beacon beam (n^*,m^*) and the center of the camera's FoV $\left(\frac{N'}{2},\frac{M'}{2}\right)$, is

$$\begin{cases} \delta_x = n^* - \frac{N'}{2}, \\ \delta_y = m^* - \frac{M'}{2}. \end{cases}$$
 (2)

4) **PID Controll**: The controller then calculates the angular velocity of the gimbal $v=(v_x,v_y)$ based on the PID algorithm, i.e.,

$$\begin{bmatrix} v_{x} \\ v_{y} \end{bmatrix} = \mathbf{k}_{p} \begin{bmatrix} \delta_{x} \\ \delta_{y} \end{bmatrix} + \mathbf{k}_{i} \begin{bmatrix} \int \delta_{x} dt \\ \int \delta_{y} dt \end{bmatrix} + \mathbf{k}_{d} \begin{bmatrix} \frac{d\delta_{x}}{dt} \\ \frac{d\delta_{y}}{dt} \end{bmatrix}$$

$$= \mathbf{k}_{p} \begin{bmatrix} \delta_{x}^{t} \\ \delta_{y}^{t} \end{bmatrix} + \mathbf{k}_{i} \begin{bmatrix} (\delta_{x}^{t} + \delta_{x}^{t-1} + \dots + \delta_{x}^{t-w_{1}}) \Delta T \\ (\delta_{y}^{t} + \delta_{y}^{t-1} + \dots + \delta_{y}^{t-w_{1}}) \Delta T \end{bmatrix}$$

$$+ \mathbf{k}_{d} \begin{bmatrix} \frac{\delta_{x}^{t} - \delta_{x}^{t-w_{2}}}{\Delta T} \\ \frac{\delta_{y}^{t} - \delta_{y}^{t-w_{2}}}{\Delta T} \end{bmatrix} , \qquad (3)$$

where k_p , k_i , and k_d are the 2×2 matrices representing the proportional, integral, and derivative gains in the Pan and Tilt directions, respectively, which are estimated based on the field test, (δ_x^t, δ_y^t) and $(\delta_x^{t-i}, \delta_y^{t-i})$ are the current and previous i^{th} displacement measurement, respectively, w_1 and w_2 are the time window size to calculate the integral and derivative of the displacement, respectively, and ΔT is the response time of the ATP system, i.e., the period between two displacement measurements. The derived angular velocity $v = (v_x, v_y)$ will be sent to the gimbal to adjust its axes accordingly.

The four functions have low complexity, and each of them can be executed by the server (Dell XPS-8930 with i7-8700 CPU and 16 GB RAM) in less than 1 ms. The execution time can be further reduced if a more powerful server or a dedicated hardware (e.g., an FPGA board) is applied. Hence, the response time of the ATP system ΔT is mainly determined by the response time of the camera system, which is defined as the minimum delay of a motion clip that can be clearly captured and transmitted to the controller. The response time of the camera system of our designed testbed, which will be described in Section IV, is 19 ms.

Note that the displacement $\boldsymbol{\delta}=(\delta_x,\delta_y)$ measured based on Eq. (2) is different from the displacement $\boldsymbol{d}=(d_x,d_y)$ between the center of the optical beam at the FSO receiver and the center of the FSO receiver's aperture (as illustrated in Fig. 1). However, $\boldsymbol{\delta}$ can be easily mapped into \boldsymbol{d} based on

$$\begin{cases} \frac{d_x}{2l \tan \frac{\theta_x}{2}} = \frac{\delta_x}{N'} \\ \frac{d_y}{2l \tan \frac{\theta_y}{2}} = \frac{\delta_y}{M'} \end{cases} \Rightarrow \begin{cases} \frac{d_x}{l} = \underbrace{\frac{2\delta_x \tan \frac{\theta_x}{2}}{N'}}, \\ \text{Angle of displacement in Pan } \epsilon_x \\ \frac{d_y}{l} = \underbrace{\frac{2\delta_y \tan \frac{\theta_y}{2}}{M'}}, \\ \text{Angle of displacement in Tilt } \epsilon_y \end{cases}$$

where l is the distance between the FSO transmitter and FSO receiver, and θ_x and θ_y are the angle of the FoV for the camera in the Pan and tilt directions, respectively, as shown in Fig. 3. Given $\boldsymbol{\delta}$ and $\boldsymbol{\theta} = (\theta_x, \theta_y)$, it is easy to derive that \boldsymbol{d} increases as l increases based on Eq. (4). Here, we define $\epsilon_x = \frac{2\delta_x \tan \frac{\theta_x}{2}}{N}$ and $\epsilon_y = \frac{2\delta_y \tan \frac{\theta_y}{2}}{N}$ as the angle of displacement in the Pan and Tilt directions, respectively, and apply ϵ_x and ϵ_y to indicate the pointing error for our designed ATP system. Note that ϵ_x and ϵ_y do not change with respect to l.

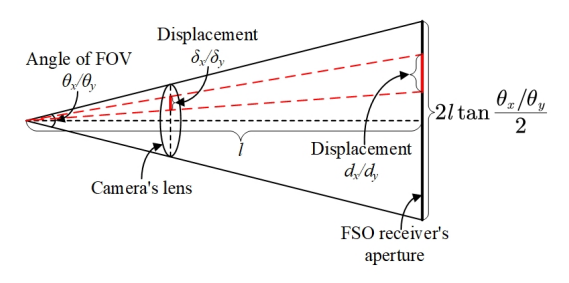


Fig. 3: Mapping from δ into d.

IV. EXPERIMENTAL EVALUATION

We will evaluate the performance of the designed ATP system by setting up a small scale testbed. As shown in Fig. 4, at the drone side, in order to accurately control the movement of the beacon/drone, we mount a beacon on a high-accuracy rotation stage. The beacon signal is first reflected by a wall, and then propagates to the camera on the WAP. Since the beacon is placed very close to the wall, we assume that the beacon signal is transmitted from the wall. As compared to the method of emitting beacon signal directly to the WAP without being reflected by the wall (which is difficult to accurately control the movement of the beacon), our design can accurately control the movement of the beacon/drone on the wall by adjusting the rotation angle and speed of the rotation stage. At the WAP side, a camera and a laser source are mounted on a DJI gimbal, where the lase source is to emulate the optical beam carrying data to the drone², and the camera is to capture the FOV image containing the beacon signal and send the captured image to the controller via the video capture card. The controller is to process the captured image and calculate the angular velocity of the gimbal.

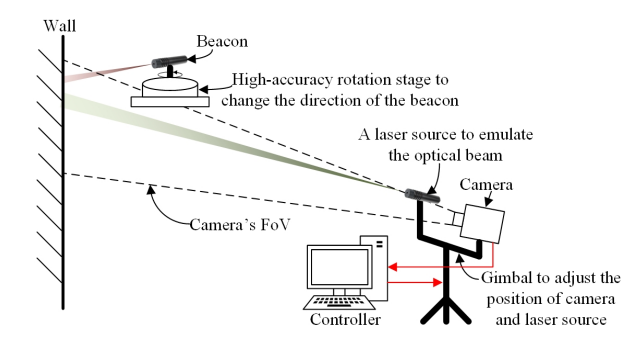


Fig. 4: The configuration of the ATP testbed.

TABLE I: Equipment in the testbed

Name	Equipment
Camera	Sony AX-53
Beacon	10mW 650nm
Gimbal (for camera and laser source)	DJI Ronin-S
Rotation stage (for beacon)	Thorlabs DDR100
Controller	Dell XPS-8930

TABLE II: Experiment parameters

Parameter	Value
Proportional gain (k_p)	[1.075,0;0,1.15]
Integral gain (k_i)	[1.925,0;0,2.443]
Derivative gain (k_d)	[0.19,0;0,0.172]
Original resolution of the camera $(M \times N)$	1280×720
Down sampling factor (κ)	5
Angle of FoV in Pan and Tilt (θ_x and θ_y)	9.85 and 5.54 mrad
Time window for the displacement integral (w_1)	76ms
Time window for the displacement derivative (w_2)	19ms

²Note that the laser source in the experiment is to visually demonstrate the laser beam on the wall can be adjusted corresponding to the movement of the beacon on the wall. It is not used for measuring the pointing error. Please check the video via the link below for the demo. https://drive.google.com/file/d/1N3q4WA1zX1BzFhVMNIX5vgT7W9_YS08g/view?usp=sharing.



Fig. 5: The designed ATP testbed.

We move the beacon on the wall by adjusting the rotation stage and calculate (ϵ_x,ϵ_y) based on Eq. (4) during every time interval $\Delta T=19$ ms. In each round, the beacon on the wall follows a line trajectory with the angle of 0.7328 rad, where the beacon moves from the original to ending points of the line with velocity k m/s, and then reverses back to the original point with velocity -k m/s, where a negative velocity represents a reverse direction. The beacon keeps following the same trajectory but increasing velocity k from 1 to 14 m/s over rounds. So, in each round, there are two acceleration periods (from 0 to k/-k m/s) and two deceleration periods (from k/-k m/s to 0) with 35/-35 m/s² acceleration/deceleration. The corresponding demo video can be found in Footnote 2.

Figs. 6 and 7 show the angle of displacement over time when v=2 m/s and v=10 m/s, respectively. From the figures, we can find that the angle of displacement ϵ_x/ϵ_y for the designed ATP system oscillates when the beacon velocity k does not change, and ϵ_x/ϵ_y may significantly change when the beacon is in the acceleration and deceleration periods. In addition, ϵ_x/ϵ_y is the minimum when k=0 and increases as k increases. For example, $|\epsilon_x|$ is always less than 1 mrad when k=2 m/s in Fig. 6. Yet, $|\epsilon_x|$ is mostly larger than 2 mrad when k=10 m/s in Fig. 7. Moreover, the angle of displacement in Pan (i.e., $|\epsilon_x|$) is smaller than that in Tilt (i.e., $|\epsilon_y|$). This is probably because the mechanical design of the DJI Ronin-S gimbal, where the Pan axis is much stable than the Tilt axis, thus having higher accurate control.

To avoid the performance uncertainty during the acceleration and deceleration periods, we measure the angle of displacement $|\epsilon_x|$ and $|\epsilon_y|$ when the beacon is in a constant speed. Figs. 8 and 9 are the box plots of the angle of displacement in the Pan and Tilt directions, respectively, under different constant speeds. The results in the figures demonstrate that $|\epsilon_x|$ and $|\epsilon_y|$ increase as k increases. Based on the results in Figs. 8 and 9, we then calculate the average displacement $\|d\|$ between the center of the optical beam at the FSO receiver and the center of the FSO receiver's aperture (as shown in Fig. 1) by varying the distance l and beacon velocity k, where

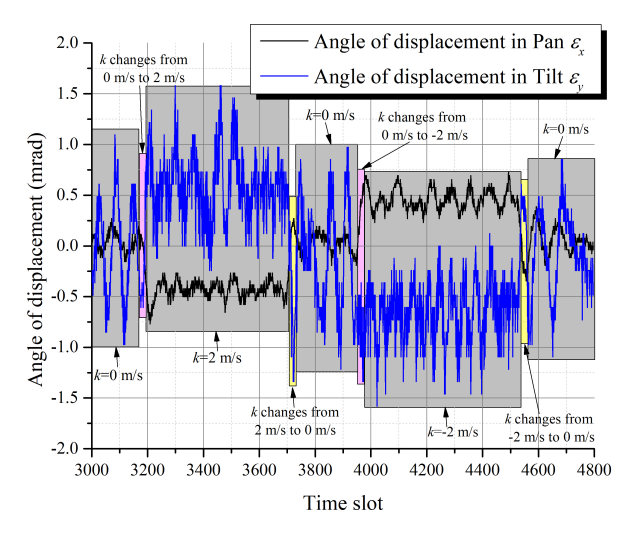


Fig. 6: The angle of displacement when k = 2 m/s.

 $\|\boldsymbol{d}\| = \sqrt{\left(d_x\right)^2 + \left(d_y\right)^2}$, and d_x and d_y are calculated based on Eq. (4). It is not surprising to see that the displacement $\|\boldsymbol{d}\|$ is monotonically increasing with respect to the beacon velocity k and distance l between the drone and the WAP.

We further analyze the average pointing loss of the FSO link by applying the designed ATP system. Normally, the pointing loss can be estimated by [27]

$$h^{poi} = \exp\left(-\frac{2\sqrt{2}d^2\rho^{rx}\exp\left(-\frac{\pi(\rho^{rx})^2}{2(\rho^{rx_beam})^2}\right)}{(\rho^{rx_beam})^3\operatorname{erf}\left(\frac{\sqrt{\pi}\rho^{rx}}{\sqrt{2}\rho^{rx_beam}}\right)}\right), \quad (5)$$

where ρ^{rx} and ρ^{rx_beam} are the radii of the FSO receiver's aperture and the optical beam at the FSO receiver's aperture, respectively, as illustrated in Fig. 1, and erf() is the Gauss error function. Normally, $\rho^{rx_beam} \approx l \times \frac{\zeta}{2}$, where ζ is the divergence angle of the optical beam. Assuming $\rho^{rx}=5$ cm, Figs. 11, 12, and 13 show the value of h^{poi} by applying the designed ATP system when ζ equals 2, 1, and 0.1 mrad, respectively. From the figures, we can find that given l, h^{poi} is monotonically non-increasing as k increases³, which is easy to understand since the displacement $\|d\|$ increases once k increases. However, it is interesting to observe that given beacon velocity k, the changes of h^{poi} over distance l is complicated, depending on the divergence angle ζ . For example, in Fig. 11, h^{poi} is monotonically non-decreasing as l increases given k. This is because if a large divergence angle $\zeta=2$ mrad is applied, the radius of the optical beam ρ^{rx_beam} increases much faster than $\|d\|$ over l, and so a larger ρ^{rx_beam} can reduce the pointing loss caused by the displacement. On the other hand, if a smaller divergence angle $\zeta = 0.1$ mrad is applied, as shown in Fig. 13, ρ^{rx_beam} increases much slower than $\|d\|$ over l, and so a larger ρ^{rx_beam} cannot reduce the pointing loss anymore. Hence, h^{poi} is monotonically nondecreasing as the distance l increases given k.

From Figs. 11-13, we can also derive that the designed ATP system is enough to generate low pointing loss to establish the

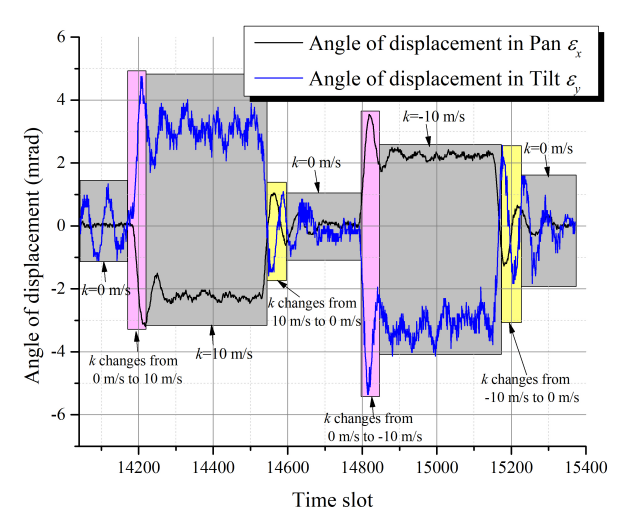


Fig. 7: The angle of displacement when k = 10 m/s.

FSO based fronthaul link when 1) a large divergence angle optical beam is applied to carry data and the velocity of the drone, i.e., k, is not high (e.g., less than 5 m/s) as shown in Fig. 11, or 2) a small divergence angle optical beam is used and the distance between the drone and the WAP is short (e.g., less than 400 m) as shown in Fig. 13. Otherwise, a fine-tuned ATP system is needed to reduce the pointing errors.

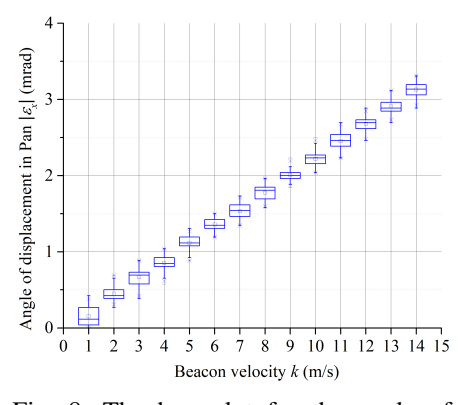
V. CONCLUSION

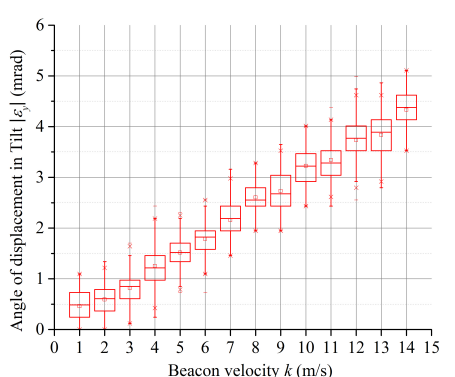
In this paper, we have designed a cost effective and lightweight ATP system for the FSO based fronthaul link in drone assisted wireless networks. We have developed a fast but accurate image processing algorithm to derive the relative position of the drone, and employed PID to control the gimbal. We have experimentally evaluated the performance of the ATP system, which can achieve low pointing loss, especially when the drone is in a low speed with proper beam divergence angle.

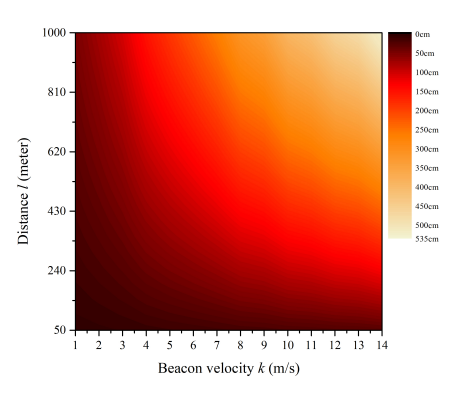
REFERENCES

- D. Wu, X. Sun, and N. Ansari, "An fso-based drone charging system for emergency communications," *IEEE Transactions on Vehicular Tech*nology, vol. 69, no. 12, pp. 16155–16162, 2020.
- [2] —, "A cooperative drone assisted mobile access network for disaster emergency communications," in 2019 IEEE Global Communications Conference (GLOBECOM), 2019, pp. 1–6.
- [3] S. Zhang, X. Sun, and N. Ansari, "Placing multiple drone base stations in hotspots," in 2018 IEEE 39th Sarnoff Symposium, 2018, pp. 1–6.
- [4] X. Li, "Deployment of drone base stations for cellular communication without apriori user distribution information," in 2018 37th Chinese Control Conference (CCC), 2018, pp. 7274–7281.
- [5] P. V. Klaine, J. P. Nadas, R. D. Souza, and M. A. Imran, "Distributed drone base station positioning for emergency cellular networks using reinforcement learning," *Cognitive computation*, vol. 10, no. 5, pp. 790– 804, 2018.
- [6] J. P. Lemayian and J. M. Hamamreh, "First responder drones for critical situation management," in 2019 Innovations in Intelligent Systems and Applications Conference (ASYU), 2019, pp. 1–6.
- [7] D. Wu, X. Sun, and N. Ansari, "An fso-based drone assisted mobile access network for emergency communications," *IEEE Transactions on Network Science and Engineering*, vol. 7, no. 3, pp. 1597–1606, 2020.
- [8] X. Sun and N. Ansari, "Latency aware drone base station placement in heterogeneous networks," in 2017 IEEE Global Communications Conference, Dec 2017, pp. 1–6.

 $^{^{3}}$ Note that a smaller value of h^{poi} indicates a larger pointing loss.



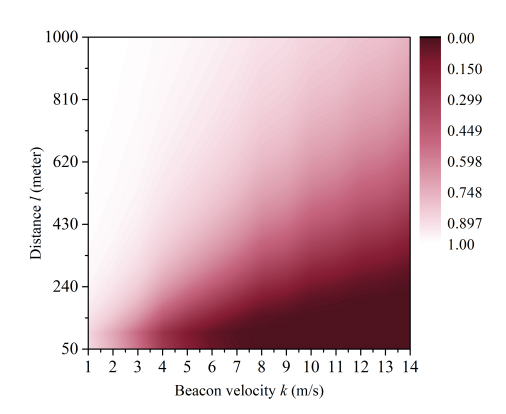


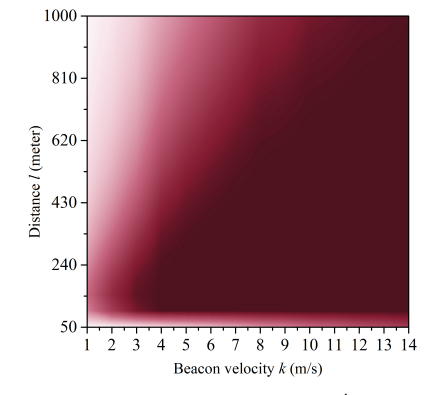


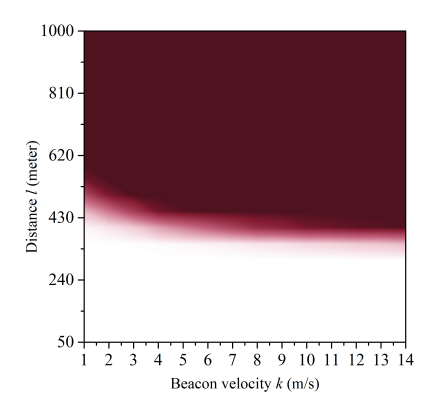
displacement in Pan.

displacement in Tilt.

Fig. 8: The box plot for the angle of Fig. 9: The box plot for the angle of Fig. 10: Average displacement $\|d\|$ by varying l and k.







mrad.

 $\zeta = 1$ mrad.

Fig. 11: Average value of h^{poi} when $\zeta = 2$ Fig. 12: Average value of h^{poi} when Fig. 13: Average value of h^{poi} when $\zeta = 0.1$ mrad.

- [9] L. Yu, X. Sun, S. Shao, Y. Chen, and R. Albelaihi, "Backhaul-aware drone base station placement and resource management for fso based drone assisted mobile networks," arXiv:2112.12883, 2021.
- [10] M. Najafi, H. Ajam, V. Jamali, P. D. Diamantoulakis, G. K. Karagiannidis, and R. Schober, "Statistical modeling of fso fronthaul channel for drone-based networks," in IEEE Intl. Conf. Commun., 2018, pp. 1-7.
- [11] S. A. Al-Ahmed, M. Z. Shakir, and S. A. R. Zaidi, "Optimal 3d uav base station placement by considering autonomous coverage hole detection, wireless backhaul and user demand," Journal of Communications and Networks, vol. 22, no. 6, pp. 467-475, 2020.
- [12] E. Ciaramella, Y. Arimoto, G. Contestabile, M. Presi, A. D'Errico, V. Guarino, and M. Matsumoto, "1.28-Tb/s (32 × 40 Gb/s) free-space optical wdm transmission system," IEEE Photonics Technology Letters, vol. 21, no. 16, pp. 1121-1123, Aug 2009.
- [13] M. Curran, M. S. Rahman, H. Gupta, K. Zheng, J. Longtin, S. R. Das, and T. Mohamed, "FSONet: A wireless backhaul for multi-gigabit picocells using steerable free space optics," in Proceedings of the 23rd Annual International Conference on Mobile Computing and Networking. New York, NY, USA: ACM, 2017, pp. 154–166.
- [14] M. A. Esmail, A. Ragheb, H. Fathallah, and M. Alouini, "Investigation and demonstration of high speed full-optical hybrid FSO/fiber communication system under light sand storm condition," IEEE Photonics Journal, vol. 9, no. 1, pp. 1-12, Feb 2017.
- [15] N. Ansari, D. Wu, and X. Sun, "Fso as backhaul and energizer for drone-assisted mobile access networks," ICT Express, vol. 6, no. 2, pp. 139-144, 2020.
- [16] H. Zhang, Y. Dong, J. Cheng, M. J. Hossain, and V. C. M. Leung, "Fronthauling for 5G LTE-U ultra dense cloud small cell networks," IEEE Wireless Communications, vol. 23, no. 6, pp. 48-53, Dec. 2016.
- [17] F. Aveta, H. H. Refai, P. LoPresti, S. A. Tedder, and B. L. Schoenholz, "Independent component analysis for processing optical signals in support of multi-user communication," in Free-Space Laser Communication and Atmospheric Propagation XXX, vol. 10524. International Society

- for Optics and Photonics, 2018, p. 105241D.
- [18] T. Zhang, X. Sun, and C. Wang, "On optimizing the divergence angle of an fso-based fronthaul link in drone-assisted mobile networks," IEEE Internet of Things Journal, vol. 9, no. 9, pp. 6914-6921, 2022.
- A. K. Majumdar, Advanced free space optics (FSO): a systems approach. Springer, 2014, vol. 186.
- A. Carrasco-Casado, R. Vergaz, J. M. Sánchez-Pena, E. Otón, M. A. Geday, and J. M. Otén, "Low-impact air-to-ground free-space optical communication system design and first results," in 2011 Intl. Conf. Space Opt. Syst. and Appl. (ICSOS), 2011, pp. 109-112.
- [21] Y. Kaymak, R. Rojas-Cessa, J. Feng, N. Ansari, M. Zhou, and T. Zhang, "A survey on acquisition, tracking, and pointing mechanisms for mobile free-space optical communications," IEEE Communications Surveys & Tutorials, vol. 20, no. 2, pp. 1104-1123, 2018.
- N. Hamedazimi, Z. Qazi, H. Gupta, V. Sekar, S. R. Das, J. P. Longtin, H. Shah, and A. Tanwer, "Firefly: A reconfigurable wireless data center fabric using free-space optics," vol. 44, no. 4, p. 319-330, aug 2014.
- [23] H. Willebrand and B. S. Ghuman, Free space optics: enabling optical connectivity in today's networks. SAMS publishing, 2002.
- H.-Y. Liu, X.-H. Tian, C. Gu, P. Fan, X. Ni, R. Yang, J.-N. Zhang, M. Hu, J. Guo, X. Cao, X. Hu, G. Zhao, Y.-Q. Lu, Y.-X. Gong, Z. Xie, and S.-N. Zhu, "Drone-based entanglement distribution towards mobile quantum networks," Natl. Sci. Rev., vol. 7, no. 5, pp. 921-928, 2020.
- K. Mori, M. Terada, K. Nakamura, R. Murakami, K. Kaneko, F. Teraoka, D. Yamaguchi, and S. Haruyama, "Fast handover mechanism for high data rate ground-to-train free-space optical communication system," in 2014 IEEE Globecom Workshops (GC Wkshps), 2014, pp. 499-504.
- [26] W. Gappmair, S. Hranilovic, and E. Leitgeb, "Performance of ppm on terrestrial fso links with turbulence and pointing errors," IEEE Communications Letters, vol. 14, no. 5, pp. 468-470, 2010.
- A. A. Farid and S. Hranilovic, "Outage capacity optimization for free-space optical links with pointing errors," Journal of Lightwave Technology, vol. 25, no. 7, pp. 1702-1710, 2007.